Molecular Crystals and Liquid Crystals
Publication details, including instructions for authors and subscription information:
http://www.tandfonline.com/loi/gmcl16

Dielectric Regime of Electrohydrodynamic Instability in Nematic Liquid Crystals

M. I. Barnik [a], L. M. Blinov [a], M. F. Grebenkin [a] & A. N. Trufanov [a]
[a] Organic Intermediates and Dyes Institute, Moscow, U.S.S.R.
Version of record first published: 21 Mar 2007.

To cite this article: M. I. Barnik , L. M. Blinov , M. F. Grebenkin & A. N. Trufanov (1976): Dielectric Regime of Electrohydrodynamic Instability in Nematic Liquid Crystals, Molecular Crystals and Liquid Crystals, 37:1, 47-56

To link to this article: http://dx.doi.org/10.1080/15421407608084345

Mol. Cryst. Liq. Cryst., 1976, Vol. 37, pp. 47–56

Printed in Holland

Dielectric Regime of Electrohydrodynamic Instability in Nematic Liquid Crystals

M. I. BARNIK, L. M. BLINOV, M. F. GREBENKIN, and A. N. TRUFANOV

Organic Intermediates and Dyes Institute, Moscow, U.S.S.R.

(*Received August 23, 1976*)

The frequency dependencies of the threshold voltage of electrohydrodynamic instability in nematic liquid crystals were investigated as functions of the dielectric anisotropy ($-1.5 < \varepsilon_a < +10$), electric conductivity ($10^{-11} < \sigma < 5.10^{-9}$ ohm^{-1}cm^{-1}) and anisotropy of the conductivity ($1.1 < \sigma_{\parallel}/\sigma_{\perp} < 1.8$). Three types of the instability have been considered: a) for $\varepsilon_a < 0$ and the planar orientation at the frequencies above the critical one ("chevron" or dielectric regime); b) for $\varepsilon_a > 0$ and the homeotropic orientation at all the frequencies (the circular and fingerprint-type domains); c) in the isotropic phase. The threshold voltage in the nematic phase was shown to be independent of the anisotropy parameters and the orientation of a liquid crystal and to coincide with the threshold of the instability in the isotropic phase. Thus, we came to the conclusion that the instability has the isotropic character in all the cases investigated.

1 INTRODUCTION

It is well known[1,2] that above the critical voltage an electrohydrodynamic (EHD) instability arises in thin layers (thickness $d \approx 10$–$100\ \mu$) of nematic liquid crystals (NLCs) with positive anisotropy of electrical conductivity ($\sigma_{\parallel}/\sigma_{\perp} > 1$). Four main cases may be differentiated:

1) For negative dielectric anisotropy ($\varepsilon_a = \varepsilon_{\parallel} - \varepsilon_{\perp} < 0$) and the planar orientation of NLCs the instability appears in the form of Williams domains at the frequencies lower than the critical one ($f < f_c$) and in the form of "chevrons" at the frequencies $f > f_c$. In that case the critical frequency

$$f_c = \frac{\omega_c}{2\pi} = \frac{\xi^2 - 1}{2\pi\tau_{\parallel}} \tag{1}$$

depends on "longitudinal" time of dielectric relaxation ($\tau_{\parallel} = \varepsilon_{\parallel}/4\pi\sigma_{\parallel}$) and the anisotropy parameter ξ^2, which for one-dimensional model[3,4] may be written as follows

$$\xi^2 = \left(1 - \frac{\sigma_\perp}{\sigma_\parallel} \cdot \frac{\varepsilon_\parallel}{\varepsilon_\perp}\right)\left(1 + \frac{\alpha_2}{\eta_2} \cdot \frac{\varepsilon_\parallel}{\varepsilon_a}\right) \tag{2}$$

where $\eta_2 = 1/2(-\alpha_2 + \alpha_4 + \alpha_3)$ and α_i are Leslie coefficients.[1]

2) For $\varepsilon_a < 0$ and the homeotropic orientation the same instability appears through the intermediate stage of reorientation of the director since usually the reorientation threshold is rather low, of the order of few volts (in the opposite case, i.d., for $\varepsilon_a \approx 0$, the instability at low frequencies arises in the form of the square grid with large wave vector[5]).

3) For $\varepsilon_a > 0$ and the homeotropic orientation Williams domains do not appear, however, at high enough voltages another type of EHD instability in the form of circular domains[6] takes place.

4) In the case $\varepsilon_a > 0$ and the planar orientation the stationary Williams domains exist for small values of ε_a only, when the threshold of EHD instability is lower than the threshold of reorientation.[5] For large values of ε_a first of all the Freedericks transition is observed then, with increasing voltage, the stationary EHD instability in the form of complex domain pattern arises.[7]

The experimental dependencies of the threshold voltage (U_{th}) of Williams domains (the conductance regime of EHD instability, $f < f_c$) on NLC anisotropy parameters (ε_a, $\sigma_\parallel/\sigma_\perp$) both for $\varepsilon_a < 0$ and $\varepsilon_a > 0$[5,8] agree well with two-dimensional theory of Pikin and Penz[9,10] based on the Helfrich model.[3] One-dimensional theory of the "chevron" threshold (dielectric regime of the instability, $f > f_c$) for the planar orientation[4,11] and $\varepsilon_a < 0$ predicts rather strong dependence of U_{th} on anisotropy parameter ξ^2, i.d. on ε_a and $\sigma_\parallel/\sigma_\perp$. As far as we know, this theory was not still verified experimentally. The mechanism of instability in the case of $\varepsilon_a > 0$ and homeotropic orientation has not theoretically treated at all (in Ref. 12 this situation has been considered to be the stable one). Kirsanov was first who noticed the resemblance between the voltage-frequency curves ($U_{th} \sim f^{1/2}$) for the instabilities in the nematic (for both $\varepsilon_a < 0$ and $\varepsilon_a > 0$) and the isotropic phases,[7] however, he did not make any quantitative measurements.

The purpose of this paper was to relate the electrical parameters of NLCs (σ, $\sigma_\parallel/\sigma_\perp$, ε_a) to the threshold field of EHD instabilities arising under following conditions:

a) at $f > f_c$ in the case of $\varepsilon_a < 0$ and the planar orientation ("chevron" or dielectric regime[11]);

b) at the frequencies $f < f_c$ and $f > f_c$ for $\varepsilon_a > 0$ and the homeotropic orientation;

c) in the isotropic phase.

In this way we hoped to understand better the possible mechanism of these instabilities.

2 EXPERIMENTAL TECHNIQUE

We investigated the threshold voltage of EHD instability (U_{th}) in standard cells of thickness 20 μ as a function of frequency of sinusoidal voltage in the range 20 Hz $< f <$ 10 KHz. The square-wave pulses (for which the theory[11] has been developed) were also used and U_{th} was shown to be practically independent of the form of the driving voltage and determined by its r.m.s. value. The curves $U_{th}(f)$ were measured for NLCs with different dielectric anisotropy ($-1.5 < \varepsilon_a < +10$), electrical conductivity ($10^{-11} < \sigma_{\parallel} < 5.10^{-9}$ ohm^{-1}cm^{-1}) and anisotropy of the conductivity ($1.1 < \sigma_{\parallel}/\sigma_{\perp} < 1.8$) oriented both homogeneously and homeotropically (the values of σ, $\sigma_{\parallel}/\sigma_{\perp}$ have been given for $f = 1$ kHz[5]).

The value of ε_a was changed by doping MBBA using the compounds with large longitudinal (the *p'*-cyanophenyl ester of *p*-heptylbenzoic acid, CEHBA) and large transverse (the 2,3-dicyano-4-amyloxyphenyl ester of *p*-amyloxybenzoic acid, DCEAA) dipole moments. The electric conductivity and anisotropy of the conductivity were varied by doping MBBA with the ionic (tetrabutyl ammonium bromide, TBAB) or the acceptor (tetracyanoethylene, TCE) impurities.[5] The mixture of azoxycompounds (mixt. A,[5] doped with CEHBA or DCEAA) as well as the pure 4-*p*-hexyl-4'-cyanobiphenyl (HCBP) having the nematic interval 16–30°C and $\varepsilon_a = +10$ ($t = 20$°C) were also used. To obtain the planar orientation SnO_2-coated electrodes were rubbed in one direction. The careful mechanical and chemical purification of the SnO_2 electrodes was used to cause the homeotropic alignment of all the liquid crystals.

The appearance of instability in the isotropic phase was registrated by microscopic observation of the circular movement of dust particles. In the nematic phase in addition to this movement (being circular for $\varepsilon_a > 0$ and translational for $\varepsilon_a < 0$) the spatially periodical (domain) patterns were also observed under the polarization microscope. The threshold voltage can be read in an accuracy of $\pm 5\%$ and $\pm 10\%$ in the cases of the domain patterns and the particle movement, respectively. Photoelectric registration of the optical transmission of the He–Ne laser beam provides approximately the same values of U_{th} for the nematic phase as in the case of visual observations.

3 RESULTS

3.1 The case of $\varepsilon_a < 0$ and the planar orientation

The experimental frequency dependencies of the threshold voltage of Williams domains and the "chevrons" are given in Figure 1 for the mixtures (on the base of MBBA) with different ε_a and σ. Corresponding theoretical curves calculated for dielectric regime of the unstability from the formulae (34), (36) and (28) of Ref. 11 are shown in Figure 2. In the experiment we change two parameters only (σ and ε_a, i.d., ξ^2), the other ones (the viscosity, elasticity) were held to be constant.[5]

Let us look at the curves 1–4 in Figure 1 for which the value of ε_a is fixed ($\varepsilon_a = -0.5$) but the conductivity increases 20 times. We can notice the following features:

a) At the high frequencies ($f > f_c$) U_{th} is proportional to $f^{1/2}$ and independent of σ in according to the theory,[11] though the experimental data on U_{th} exceed appreciably the theoretical ones (e.g., at $f = 1$ kHz $U_{th}^{exp} = 135$ V, $U_{th}^{theor} = 74$ V).

b) The "chevrone" regime was also observed at the frequencies $f < f_c$, i.d., under conditions of co-existence with the Williams domains. For this reason the curves 2–6 branch out the critical frequency. Upper (chevron) branches have a tendency to achieve plateaus for decreasing frequency. The height of the plateaus is approximately proportional to $\sigma^{1/2}$ in accordance

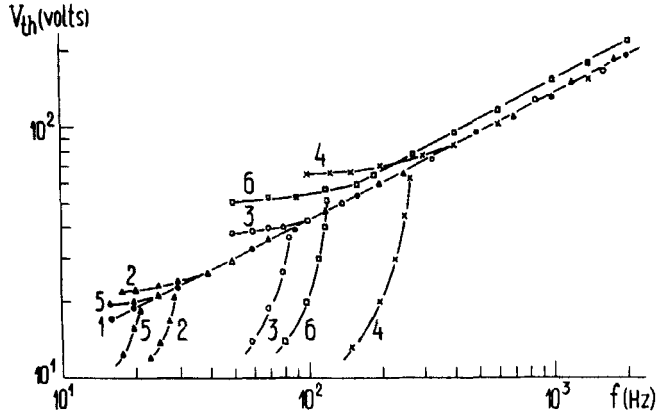

FIGURE 1 Threshold voltage of EHD instability as a function of frequency for NLCs with $\varepsilon_a < 0$ (doped MBBA, $d = 20\ \mu$, $t = 23°C$, planar orientation).

1–4 $\varepsilon_a = -0.5$, $\sigma_\parallel/\sigma_\perp = 1.3$, $\sigma_\parallel = 3 \cdot 10^{-11}$ (1), $5.5 \cdot 10^{-11}$ (2), $1.5 \cdot 10^{-10}$ (3), $5 \cdot 10^{-10}$ (4) ohm^{-1}cm^{-1};

5 $\varepsilon_a = -0.1$, $\sigma_\parallel = 4 \cdot 10^{-11}$ ohm^{-1}cm^{-1}, $\sigma_\parallel/\sigma_\perp = 1.3$;

6 $\varepsilon_a = -1.3$, $\sigma_\parallel = 2.5 \cdot 10^{-10}$ ohm^{-1}cm^{-1}, $\sigma_\parallel/\sigma_\perp = 1.38$.

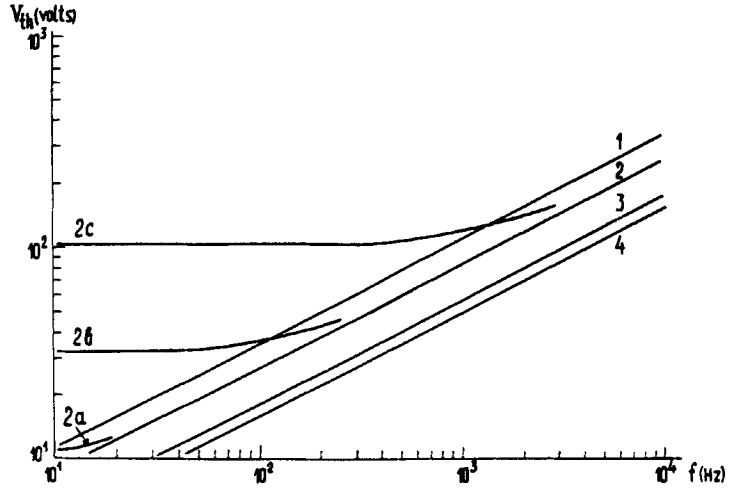

FIGURE 2 Calculated dependencies of the threshold voltage of EHD instability in the dielectric regime on frequency ($d = 20\ \mu$, $\sigma_{\parallel}/\sigma_{\perp} = 1.43$).

1, 2 High-frequency limit for the case $\xi^2 > 2.35$ [11, Eq. (34)], $\varepsilon_{\perp} = 5.25$, $\eta = 16.5$ cP, $\eta_B = 12$ cP;

1 $\varepsilon_a = -0.001$ ($\xi^2 \to \infty$);

2 $\varepsilon_a = -0.5$ ($\xi^2 = 2.65$).

3, 4 High-frequency limit for the case $\xi^2 < 2.35$ [11, Eq. (36)]

3 $\varepsilon_a = -3$ ($\xi^2 = 1.25$), $\varepsilon_{\perp} = 7.8$, $\eta = 8.1$ cP;

4 $\varepsilon_a = -5$ ($\xi^2 = 1.14$) $\varepsilon_{\perp} = 10$, $\eta = 6.5$ cP.

2(a-c) low-frequency limit for the curve 2 [11, Eq. (28)]: $\sigma_{\parallel} = 10^{-10}$ (a), 10^{-9} (b), 10^{-8} (c) ohm^{-1}cm^{-1}.

with the theory,[11] however, again the experimental values of U_{th} are 2 or 3 times larger than the theoretical ones.

The curves 2, 5, 6 in Figure 1 correspond to different value of ($\varepsilon_a = -0.5$, -0.1 and -1.5 respectively, σ being approximately equal for the curves 2 and 5). Despite of 15-fold variation of ε_a (hence, the parameter ξ^2 was changed from 8.5 to 1.5) the high-frequency parts of the corresponding experimental curves coincide practically in contrast to the theoretical curves of Figure 2 which predict the noticeable dependence U_{th} on dielectric anisotropy. We have checked also that $U_{th}(f)$ at $f > f_c$ is independent of anisotropy of the electrical conductivity. In that case the mixture A doped with TCE ($\sigma_{\parallel}/\sigma_{\perp} = 1.1$) and TBAB ($\sigma_{\parallel}/\sigma_{\perp} = 1.75$) was used. It should be noted that weak disagreement between the curve 6 and the others at $f > f_c$ is due to the enhanced viscosity of the substance being prepared by doping MBBA with 5% of DCEAA (see below). Now let us leave open the question about the discrepancy between the experimental and theoretical data and discuss the instability for $\varepsilon_a > 0$.

3.2 The case $\varepsilon_a > 0$ and the homeotropic orientation

The threshold voltages of EHD instability for NLCs with different values of σ and $\varepsilon_a > 0$ are shown in Figure 3. The curves in Figure 3 are very like to the "chevron" branches of Figure 1, however, for the case $\varepsilon_a > 0$ the low-frequency plateaus are very much more pronounced since the instability is not masked by Williams domains. The instability appears in the form of "fingerprints" at the frequencies $f < f_c$ (plateau region, Figure 4a) and in the form of the conoscopic crosses or circular domains[6] at $f > f_c$, Figure 4b. The dust particles move either along domain loops or around the noddes in the former case but in the latter one they move around the crosses only (in clockwise or counter-clockwise directions).

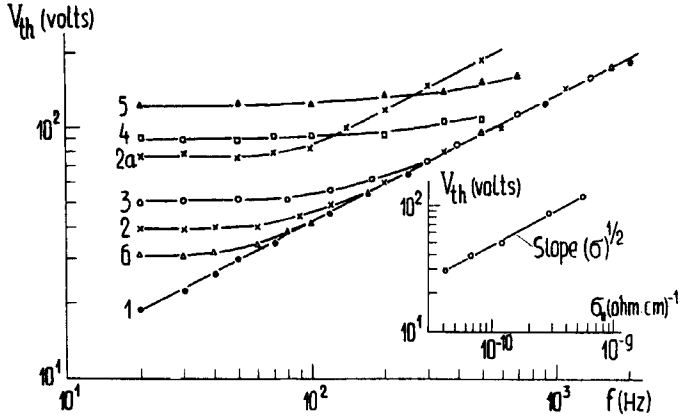

FIGURE 3 Threshold voltage of EHD instability as a function of frequency for NLCs with $\varepsilon_a > 0$ (doped MBBA, $t = 23°C$, $\sigma_{\parallel}/\sigma_{\perp} = 1.3$, homeotropic orientation).

1–5 $\varepsilon_a = 0.1$, $\sigma_{\parallel} = 4 \cdot 10^{-11}$ (1), $7 \cdot 10^{-10}$ (2), $1.2 \cdot 10^{-9}$ (3), $3 \cdot 10^{-9}$ (4), $5.5 \cdot 10^{-9}$ (5) ohm^{-1}cm^{-1}, $d = 20\ \mu$; $\sigma_{\parallel} = 7 \cdot 10^{-10}$ ohm^{-1}cm^{-1}, $d = 40\ \mu$ (2a).

6 $\varepsilon_a = 3$, $\sigma_{\parallel} = 8 \cdot 10^{-10}$ ohm^{-1}cm^{-1}.

Inset—Low-frequency threshold voltage as a function of the electric conductivity ($f = 20$ Hz, $d = 20\ \mu$).

The following features need to be commented.

a) As in the case $\varepsilon_a < 0$ the instability has *a field threshold*, i.d., U_{th} increases linearly with increasing thickness of cells (see the curves 2 and 2a in Figures 3 and Ref. 13). Besides, at high frequencies $U_{th} \sim f^{1/2}$.

b) With increasing σ the low-frequency threshold increases according to the law $U_{th} \sim \sigma^{1/2}$ (see the curves 1–5 and the inset of Figure 3).

c) The threshold voltage $U_{th}(f)$ does not change for the 30-fold change in ε_a (for the curve 6 $\varepsilon_a = +3$, for the other ones $\varepsilon_a = +0.1$). The curves $U_{th}(f)$ obtained for HCBP ($\varepsilon_a = +10$) are also in quantitative agreement

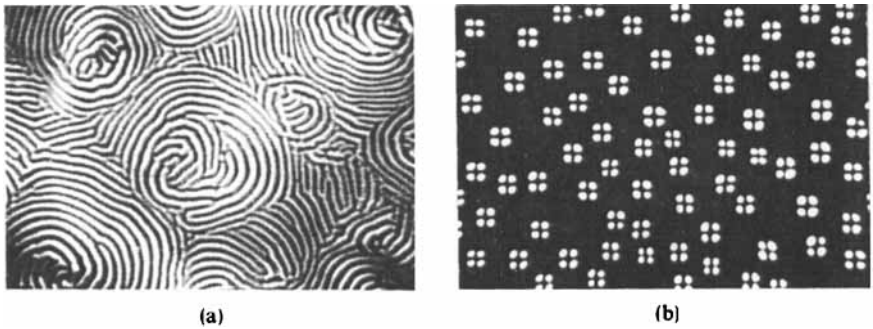

(a) (b)

FIGURE 4 Domain patterns for homeotropically oriented NLCs with $\varepsilon_a > 0$ ($d = 20\ \mu$).
(a) the "fingerprint" domains typical for the frequenceis $f < f_c$ ($\varepsilon_a = +0.1$, $\sigma_{\parallel} = 4{\cdot}10^{-10}$ ohm^{-1}cm^{-1}, $f = 30$ Hz);
(b) the circular domains for $f > f_c$ ($\varepsilon_a = +0.1$, $\sigma_{\parallel} = 4.10^{-11}$ ohm^{-1}cm^{-1}, $f = 100$ Hz).
The areas of the photographs are 1000 μ × 700 μ (a) and 600 μ × 410 μ (b).

with the curves 1–6. The high-frequency parts of the curves are also independent of the ratio $\sigma_{\parallel}/\sigma_{\perp}$.

d) The most interesting fact is that the curves $U_{th}(f)$ for the cases of $\varepsilon_a < 0$ and $\varepsilon_a > 0$ coincide very closely at the frequencies $f > f_c$ where $U_{th} \sim f^{1/2}$ (e.g., compare the curves 1 in Figures 1 and 3). The universality of the curves $U_{th}(f)$ for $\varepsilon_a < 0$ and $\varepsilon_a > 0$ as well as the independence U_{th} of the anisotropic parameters of NLCs (ε_a, $\sigma_{\parallel}/\sigma_{\perp}$, i.d., ξ^2) suggest us an idea that the instability for both $\varepsilon_a < 0$ (at $f > f_c$) and $\varepsilon_a > 0$ (at all the frequencies) has an isotropic character. To demonstrate the evidence of this mechanism we have investigated the threshold-frequency curves for the instability in the isotropic phase of pure and doped MBBA and in other non-mesomorphic liquids.

3.3 The isotropic case

It is convenient to take the measurements beginning from the homeotropically oriented nematic phase with $\varepsilon_a > 0$. In that case at $f > f_c$ one can observe under polarization microscope the circular motion of dust particles around the crosses of circular domains. The threshold voltage of the motion† coincides approximately with domain threshold and decreases with increasing temperature. At the clearing point the domain pattern disappears but the circular motion of the particles remains and U_{th} can be measured in the isotropic phase too. The curves $U_{th}(f)$ for doped MBBA ($\varepsilon_a = +0.1$ at 20°C, clearing point is 42°C) at different temperatures are given in Figure 5.

† Sometimes the particles move at the voltages below this threshold but in that case their trajectories are random.

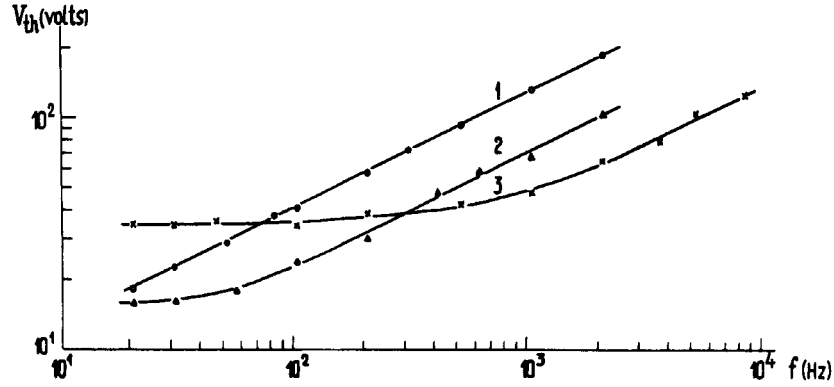

FIGURE 5 The comparison of the threshold-frequency curves for the nematic and isotropic phases (doped MBBA, $\varepsilon_a = 0.1$, $d = 20\ \mu$, initial homeotropic orientation). Temperature: 23°C (1), 41°C (2), 55°C (3).

The analogy between the dependencies $U_{th}(f)$ in the nematic and isotropic phases is evident. The appearance of well pronounced plateau (curve 3) with increasing temperature is due to the increase in the electrical conductivity of the substance.

In Figure 6 the temperature dependencies of U_{th} (at high frequencies, $f > f_c$) are shown for pure ($\varepsilon_a = -0.5$) and doped ($\varepsilon_a = +0.1$) MBBA. One

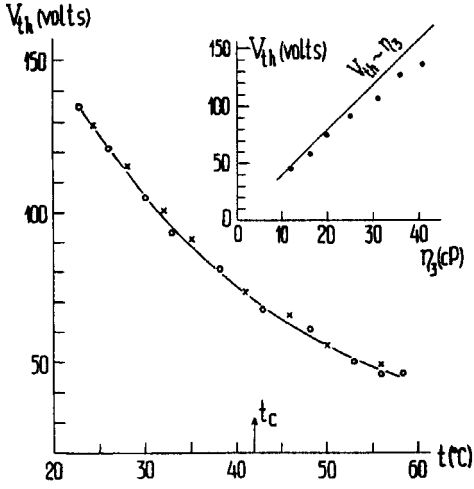

FIGURE 6 Temperature dependence of the threshold voltage in the high-frequency limit ($f = 1$ kHz).

ooo—pure MBBA, xxx—doped MBBA ($\varepsilon_a = 0.1$).

Inset—Threshold voltage vs the viscosity coefficient η_3.

can see that there is no jump in U_{th} at the transition temperature. The value of U_{th} correlates approximately with the viscosity coefficient $\eta_3 = \frac{1}{2}\alpha_4$ of MBBA taken from Ref. 14 (see inset of Figure 6).

We have observed the same instability in ordinary isotropic liquids (silicon oil, acetone and CCl_4). The threshold voltage of particle movement decreases with decreasing viscosity (at $f = 100$ Hz $U_{th} = 90$, 7 and 2 volts, respectively). It should be noted that blocking of the electrodes with thin dielectric layers does not change the value of U_{th}.

4 DISCUSSION AND CONCLUSION

Using dimensional arguments and comparing the energy of an electric field with dissipation energy $\varepsilon E^2/4\pi \sim \eta\omega$ [Ref. 1, page 196] we can write the following expressions for the threshold field which describe well all our experimental data

$$E_{th}^2 = \frac{4\pi\eta\omega}{\varepsilon} \quad (\omega \gg \omega_c) \tag{3}$$

$$E_{th}^2 = \frac{4\pi\eta}{\varepsilon\tau_0} = \frac{16\pi^2\eta\sigma}{\varepsilon^2} \quad (\omega \ll \omega_c) \tag{4}$$

Here σ, ε, η are the mean values of electrical conductivity, dielectric constant and viscosity, $\omega = 2\pi f$ (in Eq. (4) the reciprocal relaxation time τ_0^{-1} substitutes for ω in Eq. (3)).

Let us evaluate the values of U_{th}: at frequency 150 Hz ($\omega = 10^3$ sec^{-1}) for $\varepsilon = 5$, $\eta = 0.5$ P we obtain from (3) $E_{th} = 9.10^3$ V $\cdot$ cm^{-1}. i.d., for the cell of thickness $d = 20\ \mu$ $U_{th} = 18$ V (the experimental value is 50 V). At low frequencies (plateau region, $\omega \to 0$) for $\sigma = 10^{-10}$ ohm^{-1}cm^{-1} = 90 CGS units Eq. (4) gives $E_{th} = 5.1 \cdot 10^3$ V $\cdot$ cm^{-1} and $U_{th} = 10.2$ V for $d = 20\ \mu$ (the experimental value is 15 V). Thus, to some extent the formulae (3) and (4) agreed with experiment even quantitatively, though the experimental dependencies U_{th} upon viscosity and dielectric constant have to be measured more precisely.

The formula to be analogous to (4) has been derived strictly[15] for the case of stationary bipolar injection of charges in the isotropic liquid ($\omega = 0$). More general approach involving the consideration of frequency behaviour of the threshold field is developed in Ref. 13 and results in the expressions analogous to Eqs. (3) and (4) (with other numerical coefficients).

The formulae (3) and (4) being independent of the anisotropy parameters (ε_a, $\sigma_{\parallel}/\sigma_{\perp}$, K_{ii} etc) and the orientation of NLCs agree well with experimental data. Thus, we came to conclusion that the instability for the case $\varepsilon_a > 0$ at all the frequencies and for $\varepsilon_a < 0$ at $f > f_c$ (in so-called dielectric regime) as

well as in the isotropic phase has the same (isotropic) mechanism. The role of a liquid crystal is reduced only to the visualization of the instability for optical anisotropy. Of course, the form of the domain pattern depends on the NLC orientation. The planar orientation (for $\varepsilon_a < 0$ and $f > f_c$) results in "chevron" structure and the homeotropic one (for $\varepsilon_a > 0$) gives rise to the fingerprint ($f < f_c$) or circular ($f > f_c$) domains. In the isotropic phase the circular movement of the solid particles can be observed only.

Acknowledgements

We are grateful to E. A. Kirsanov for kindly supplying the detailed results of his measurements and to S. A. Pikin and V. G. Chigrinov for helpful discussions.

References

1. P. G. de Gennes, *The Physics of Liquid Crystals*, Clarendon Press, Oxford, 1974.
2. L. M. Blinov, *Uspekhi Fiz. Nauk*, **114**, 67 (1974) [Eng. transl. *Sov. Phys. Uspekhi*, **17**, 658 (1975)].
3. W. Helfrich, *J. Chem. Phys.*, **51**, 4092 (1969).
4. E. Dubois-Violette, P. G. de Gennes, and O. Parodi, *J. de physique*, **32**, 305 (1971).
5. M. I. Barnik, L. M. Blinov, M. F. Grebenkin, S. A. Pikin, and V. G. Chigrinov, *Zh. Eksp. Teor. Fiz.*, **69**, 1080 (1975).
6. E. A. Kirsanov, *Uch. zapiski Ivanovsk. Gos. Univ.* (Proc. Ivanovo State Univ.), **128**, 59 (1974).
7. R. A. Kashnow and H. S. Cole, *Mol. Cryst. Liquid Cryst.*, **23**, 329 (1973).
8. M. I. Barnik, L. M. Blinov, M. F. Grebenkin, S. A. Pikin, and V. G. Chigrinov, *Phys. Lett.*, **51A**, 175 (1975).
9. S. A. Pikin, *Zh. Eksp. Teor. Fiz.*, **60**, 1185 (1971); S. A. Pikin and A. A. Shtolberg, *Kristallografiya*, **18**, 445 (1973).
10. P. A. Penz and G. W. Ford, *Phys. Rev.* (*A*)., **6**, 414, 1676 (1972).
11. I. W. Smith, Y. Galerne, S. T. Lagerwall, E. Dubois-Violette, and G. Durand, *J. de physique*, **36**, C1-237 (1975).
12. P. G. de Gennes, *Comm. Sol. St. Phys.*, **3**, 35 (1970).
13. M. I. Barnik, L. M. Blinov, S. A. Pikin, and A. N. Trufanov (to be published in *Zh. Eksp. Teor. Fiz.*).
14. C. Gähwiller, *Mol. Cryst. Liquid Cryst.*, **20**, 301 (1973).
15. R. Turnball, *J. Phys.*(*D*)., **6**, 1755 (1973).